Efficient implementation of matrix product states to quantum circuit

Takahiro Yamamoto

April 30, 2021

1 Introduction

- Classical simulation of quantum computation with slight entanglement is known: https://arxiv.org/abs/quant-ph/0301063
- In NISQ era, efficient state preparation is desirable.
- Realizing MPS on quantum hardwares is strictly limited. This is partially due to the fact that current techniques only permit short coherent time and small numbers of computing qubits.
- Efficient preparation of W-state is useful: https://arxiv.org/abs/1502.05130
- Application to simulation of quantum system such as 1-magnon state

2 Matrix product states

Expressing the most general pure state of n interacting spin system, where each spin state is described by a two-dimensional Hilbert space, requires in general 2^n complex numbers $c_{i_1 \ldots i_n}$,

$$|\Psi\rangle = \sum_{i_1=0}^{1} \cdots \sum_{i_n=0}^{1} c_{i_1 \ldots i_n} |i_1\rangle \otimes \cdots \otimes |i_n\rangle, \tag{1}$$

where $\{|0\rangle, |1\rangle\}$ denotes a single-spin orthogonal basis.

Some specific quantum states, however, can be efficiently expressed by a classical computer whenever only a restricted amount of entanglement is present in the system.

Consider a decomposition of a pure state $|\Psi\rangle$. Let A denote a subset of the n spin states and B the rest of them. The Schmidt decomposition of $|\Psi\rangle$ with respect to the partition

$A : B$ reads

$$|\Psi\rangle = \sum_{\alpha=1}^{\chi_A} \lambda_\alpha \, |\Phi_\alpha^{[A]}\rangle \otimes |\Phi_\alpha^{[B]}\rangle \,, \tag{2}$$

where $|\Phi_\alpha^{[A]}\rangle$ is an eigenvector of the reduced matrix $\mathrm{Tr}_B \, |\Psi\rangle\langle\Psi|$ and $|\Phi_\alpha^{[B]}\rangle$ is that of $\mathrm{Tr}_A \, |\Psi\rangle\langle\Psi|$, each of which has eigenvalue $|\lambda_\alpha|^2 > 0$. The Schmidt rank χ_A can be used to quantify the entanglement of state $|\Psi\rangle$ by

$$\chi = \max_A \chi_A, \tag{3}$$

that is, by the maximal Schmidt rank over all possible bipartite splittings $A : B$.

Consider a local decomposition of the state $|\Psi\rangle$ in terms of n tensors $\Gamma^{[\ell]}$ for $\ell = 1, \cdots n$ and $n-1$ vectors $\lambda^{[1]}$ for $\ell = 1, \cdots n-1$, denoted

$$|\Psi\rangle \longleftrightarrow \Gamma^{[1]} \lambda^{[1]} \Gamma^{[2]} \lambda^{[2]} \cdots \Gamma^{[\ell]} \cdots \lambda^{[n-1]} \Gamma^{[n]}. \tag{4}$$

Here, tensor $\Gamma^{[\ell]}$ is assigned to site ℓ and has at most three indices, $\Gamma^{[\ell]i}_{\alpha\alpha'}$, where virtual indices run $\alpha, \alpha' = 1, \cdots, \chi$ and physical indices run $i = 0, 1$, whereas $\lambda^{[\ell]}$ is a vector whose components $\lambda_\alpha^{[\ell]}$ store the Schmidt coefficients of the spliting $[1 \cdots \ell]$:$[(\ell+1) \cdots n]$.

$$c_{i_1 i_2 \ldots i_n} = \sum_{\alpha_1, \cdots \alpha_{n-1}} \Gamma^{[1]i_1}_{\alpha_1} \lambda^{[1]}_{\alpha_1} \Gamma^{[2]i_2}_{\alpha_1\alpha_2} \lambda^{[2]}_{\alpha_2} \cdots \Gamma^{[n]i_n}_{\alpha_{n-1}} \tag{5}$$

Note that 2^n coefficients $c_{i_1 i_2 \ldots i_n}$ are expressed in terms of about $(2\chi^2 + \chi)n$ parameters.

More explicitly, state $|\Psi\rangle$ is expressed as

$$|\Psi\rangle = \sum_{i_1=0}^{1} \cdots \sum_{i_n=0}^{1} \sum_{\alpha_1, \cdots \alpha_{n-1}} \Gamma^{[1]i_1}_{\alpha_1} \lambda^{[1]}_{\alpha_1} \Gamma^{[2]i_2}_{\alpha_1\alpha_2} \lambda^{[2]}_{\alpha_2} \cdots \Gamma^{[n]i_n}_{\alpha_{n-1}} \, |i_1\rangle \otimes \cdots \otimes |i_n\rangle \,. \tag{6}$$

3 Overview of implementation of MPS to quantum circuit

MPS in general cannot be implemented to quantum circuit in a straightforward manner. This is due to the fact that the dimension of the virtual degrees of freedom is typically much larger than the physical dimension, $\chi \gg 2$.

To realize an MPS in a quantum platform, one intuitively needs χ-level qudits as the virtual degrees of freedom [Schon05]. However, typically χ is taken (10^2) or even larger.

One way to get around the χ-level qudits is to introduce multiple-qubit gates (see, e.g., [Huggins19, Cramer00]), where the χ-level qudits in the circuits of the MPS's are equivalently replaced by several two-level qubits. Since such a scheme contains multiple-qubit gates, one must further compile these gates to one- and two-qubit gates to implement on the realistic quantum hardware [Barenco95, Chong17].

[Ran19] proposes an algorithm that efficiently and accurately encodes a MPS with $\chi \gg 2$ into a quantum circuit consisting of only one- and two-qubit gates. The idea is to construct the unitary matrix product operators, called matrix product disentanglers (MPD's), that disentangle the targeted MPS. These MPD's form a multi-layer quantum circuit, which evolves a product state into the MPS with a high fidelity.

3.1 Matrix product disentanglers

$$|\Psi\rangle = \sum_{i_1=0}^{1} \cdots \sum_{i_n=0}^{1} \sum_{\alpha_1,\cdots\alpha_{n-1}} M^{[1]i_1}_{\alpha_1} M^{[2]i_2}_{\alpha_1\alpha_2} \cdots M^{[n]i_n}_{\alpha_{n-1}} |i_1\rangle \otimes \cdots \otimes |i_n\rangle . \tag{7}$$

Let us impose that $M^{[\ell]}$ satisfy the left-orthogonal conditions, that is

$$\sum_{\alpha_1,i_1} M^{[1]i_1}_{\alpha_1} \left(M^{[1]i_1}_{\alpha_1}\right)^* = 1, \tag{8}$$

$$\sum_{\alpha_\ell,i_\ell} M^{[\ell]i_\ell}_{\alpha_{\ell-1}\alpha_\ell} \left(M^{[\ell]i_\ell}_{\alpha'_{\ell-1}\alpha_\ell}\right)^* = \delta_{\alpha_{\ell-1}\alpha'_{\ell-1}}, \tag{9}$$

$$\sum_{i_n} M^{[n]i_n}_{\alpha_{n-1}} \left(M^{[n]i_n}_{\alpha'_{n-1}}\right)^* = \delta_{\alpha_{n-1}\alpha'_{n-1}}, \tag{10}$$

where $1 < \ell < n$.

In the case where $\chi = 2$, any left-orthogonal MPS can exactly be encoded into single-layer quantum circuit consisting of only one- and two-qubit gates.

The matrix product disentanglers (MPD) U transforms the MPS $|\Psi\rangle$ into a product state. For simplicity, we define U as

$$U |\Psi\rangle = |0\rangle^{\otimes n} \tag{11}$$

The construction of the MPD for an MPS consisting of one- and two-qubit gates, $G^{[1]}, G^{[2]}, \ldots, G^{[n]}$, is as follows

1. For n-th tensor $M^{[n]}$, we have one-qubit unitary gate $G^{[n]} = M^{[n]}$.

2. For $1 < \ell < n$, the rank-three tensor $M^{[\ell]}$ gives the component of two-qubit unitary gate $G^{[\ell]}_{0ijk} = M^{[\ell]i}_{jk}$. The components of $G^{[\ell]}_{1ijk}$ are obtained by choosing orthogonal vectors in the kernel of $M^{[\ell]}$, so they satisfy

$$\sum_{kl} G^{[\ell]}_{i'j'kl} \left(G^{[\ell]}_{ijkl}\right)^* = \delta_{i'i}\delta_{j'j}, \tag{12}$$

which gives the orthogonal conditions.

3. For the tensor $M^{[1]}$, the component of the two-qubit gate $G^{[1]}$ is $G^{[1]}_{00kl} = M^{[1]k}_{l}$. The rest components of $G^{[1]}_{ijkl}$ are the orthonormal vectors in the kernel of $M^{[1]}$. Again $G^{[1]}$ satisfies the unitary conditions Eq.

Note that here we denote $G^{[n]}_{ij} = \langle i| G^{[n]} |j\rangle$ and $G^{[\ell]}_{ijkl} = \langle ij| G^{[\ell]} |kl\rangle$.
The MPD of state Ψ is then obtained

$$U |\Psi\rangle = G^{[n]} \cdots G^{[2]} G^{[1]} |\Psi\rangle = |0\rangle^{\otimes n} \tag{13}$$

3.2 Deep quantum circuit with MPDs

MPS with $\chi > 2$ can be approximated by a deep quantum circuit that contains multiple ($\mathcal{D}$) layers of MPD's. The number of gates scales linearly with the system size and the number of layers. The encoding algorithm is as following.

1. $|\Psi_0\rangle = |\Psi\rangle$ and compute the MPS $|\tilde{\Psi}_0\rangle$ by optimally truncating the virtual bond dimensions $\chi = 2$ of $|\Psi\rangle$.

2. Construct the MPD $U_{\mathcal{D}}$, which transform $U_{\mathcal{D}} |\tilde{\Psi}_0\rangle = |0\rangle^{\otimes n}$.

3. For k-th iteration, set $|\Psi_k\rangle = U_{\mathcal{D}-k} |\Psi_{k-1}\rangle$ and compute $|\tilde{\Psi}_k\rangle$ by optimally truncating the virtual bond dimensions $\chi = 2$ of $|\Psi_k\rangle$.

4. Construct the MPD $U_{\mathcal{D}-k}$, which transform $U_{\mathcal{D}-k} |\tilde{\Psi}_k\rangle = |0\rangle^{\otimes n}$.

5. If $|\Psi_{\mathcal{D}}\rangle$ is close to $|0\rangle^{\otimes n}$, that is $|\tilde{\Psi}_{k-1}\rangle \approx |\Psi_{k-1}\rangle$, then

$$|0\rangle^{\otimes n} \approx |\Psi_{\mathcal{D}}\rangle = U_1 |\Psi_{\mathcal{D}-1}\rangle = \cdots = U_1 U_2 \cdots U_{\mathcal{D}} |\Psi\rangle \tag{14}$$

   Therefore we obtain approximation of the MPS $|\Psi\rangle$ by

$$|\Psi\rangle \approx U^{\dagger}_{\mathcal{D}} \cdots U^{\dagger}_2 U^{\dagger}_1 |0\rangle^{\otimes n} \tag{15}$$

Depth required for approximation with required fidelity.

4 Quantum states with N sites and m particles

Consider m particles hopping around on a 1D lattice with N sites.

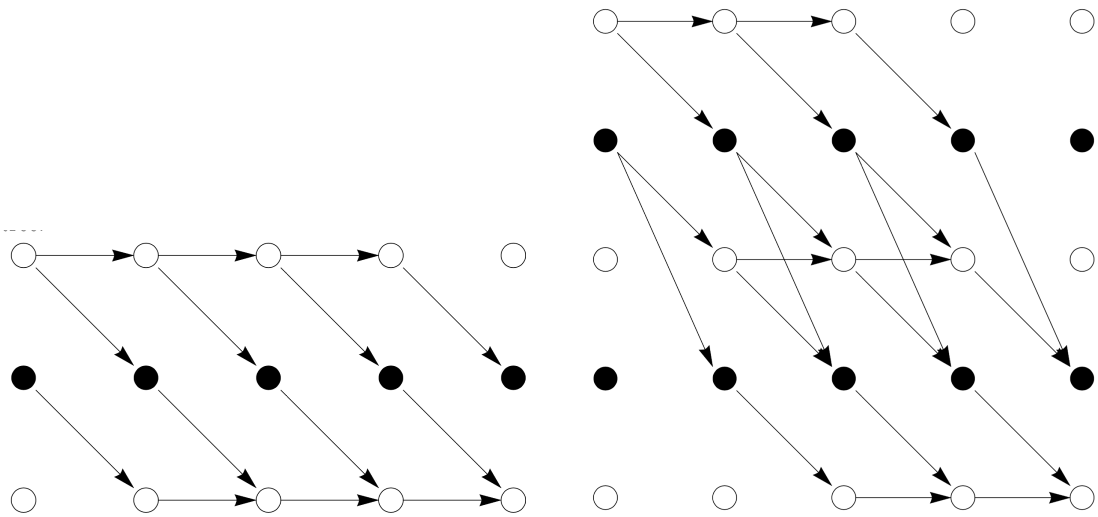

Figure 1: Diagram of one-particle state (left) and two-particle state (right)

5 (

Bond dimension)

Consider a single particle hopping around on a 1D lattice. $|\alpha_i|^2$ is the probability for the particle to be on site i. Lets algorithmically find the 1-particle basis states, starting at the left. This way of thinking will be the seed of our technique: Site 1 can be either occupied or empty. If it is empty then site 2 can be either occupied or empty. On the other hand, if site 1 was occupied, then site 2 must be empty. We get a decision tree:

Now consider the two particle problem.

The generalization to more sites and more particles should be obvious. You should be able to easily turn this into a computer algorithm for constructing m-particle states.

The bond dimension of n-site, m-particle state, k'th matrix. Each row corresponds to a different configuration of the previous $k-1$ sites, while each column corresponds to a configuration of the first k sites. We therefore just count the number of ways of putting ℓ particles on $k-1$ sites, then sum over m.

For $1 \leq k \leq n$

$$d_R = 2^{k-1} \tag{16}$$

$$d_C = 2^k \tag{17}$$

For $m < k \leq n - m$

$$d_R = 1 + \sum_{\ell=0}^{m-1} \binom{k-1}{\ell} \tag{18}$$

$$d_C = 1 + \sum_{\ell=0}^{m-1} \binom{k}{\ell} \tag{19}$$

For $n - m < k \leq n$

$$d_R = 1 + \sum_{\ell=0}^{n-k} \binom{k-1}{m+\ell-1} \tag{20}$$

$$d_C = 1 + \sum_{\ell=0}^{n-k} \binom{k}{m+\ell-1} \tag{21}$$

6 Efficient implementation of W-type state

$$|\psi_W\rangle = e^{i\varphi_1} \sin\theta_1 |0\ldots01\rangle + \cos\theta_1 e^{i\varphi_2} \sin\theta_2 |0\ldots010\rangle + \cdots + \cos\theta_1 \cdots \cos\theta_{n-2} e^{i\varphi_{n-1}} \sin\theta_{n-1} |010\ldots0\rangle + \cos\theta_1 \cdots \tag{22}$$

$$|\psi_W\rangle = \alpha_1 |0\ldots01\rangle + \alpha_1 |0\ldots010\rangle + \cdots + \alpha_{n-1} |010\ldots0\rangle + \alpha_n |10\ldots0\rangle \tag{23}$$

The MPS of non-canonical form is

$$|\Psi\rangle = \sum_{i_1=0}^{1} \cdots \sum_{i_n=0}^{1} \sum_{\alpha_1,\cdots\alpha_{n-1}} M^{[1]i_1}_{\alpha_1} M^{[2]i_2}_{\alpha_1\alpha_2} \cdots M^{[n]i_n}_{\alpha_{n-1}} |i_1\rangle \otimes \cdots \otimes |i_n\rangle . \tag{24}$$

$$M^{[1]i_1=0} = \begin{bmatrix} 1 & 0 \end{bmatrix}, M^{[1]i_1=1} = \begin{bmatrix} 0 & \alpha_1 \end{bmatrix} \tag{25}$$

$$M^{[\ell]i_\ell=0} = \begin{bmatrix} 1 & 0 \\ 0 & 1 \end{bmatrix}, M^{[\ell]i_\ell=1} = \begin{bmatrix} 0 & \alpha_\ell \\ 0 & 0 \end{bmatrix} \tag{26}$$

$$M^{[n]i_n=0} = \begin{bmatrix} 1 \\ 0 \end{bmatrix}, M^{[n]i_n=1} = \begin{bmatrix} \alpha_1 \\ 0 \end{bmatrix} \tag{27}$$

Iterate SVD from $\ell = 1$ and transofm $M^{[\ell]}$ into left-orthogonal MPS

$$\begin{bmatrix} M^{[1]i_n=0} \\ M^{[1]i_n=1} \end{bmatrix} = \begin{bmatrix} 1 & 0 \\ 0 & \alpha_1 \end{bmatrix} = \begin{bmatrix} 1 & 0 \\ 0 & 1 \end{bmatrix} \begin{bmatrix} 1 & 0 \\ 0 & \alpha_1 \end{bmatrix} \begin{bmatrix} 1 & 0 \\ 0 & 1 \end{bmatrix} \tag{28}$$

$$\Gamma^{[1]} = \begin{bmatrix} 1 & 0 \\ 0 & 1 \end{bmatrix}, \lambda^{[1]} = \begin{bmatrix} 1 \\ \alpha_1 \end{bmatrix} \tag{29}$$

$$\lambda^{[1]}V_1M^{[2]} = \begin{bmatrix} 1 & 0 \\ 0 & \alpha_1 \\ 0 & \alpha_2 \\ 0 & 0 \end{bmatrix} = \begin{bmatrix} 1 & 0 \\ 0 & \alpha_1/\sqrt{|\alpha_1|^2+|\alpha_2|^2} \\ 0 & \alpha_2/\sqrt{|\alpha_1|^2+|\alpha_2|^2} \\ 0 & 0 \end{bmatrix} \begin{bmatrix} 1 & 0 \\ 0 & \sqrt{|\alpha_1|^2+|\alpha_2|^2} \end{bmatrix} \begin{bmatrix} 1 & 0 \\ 0 & 1 \end{bmatrix} \tag{30}$$

Therefore

$$\Gamma^{[2]} = \begin{bmatrix} 1 & 0 \\ 0 & \alpha_1/\sqrt{|\alpha_1|^2+|\alpha_2|^2} \\ 0 & \alpha_2/\sqrt{|\alpha_1|^2+|\alpha_2|^2} \\ 0 & 0 \end{bmatrix}, \lambda^{[2]} = \begin{bmatrix} \frac{1}{\sqrt{|\alpha_1|^2+|\alpha_2|^2}} \end{bmatrix} \tag{31}$$

$$\mathrm{CNOT}_{21} = \begin{bmatrix} 1 & 0 & 0 & 0 \\ 0 & 0 & 0 & 1 \\ 0 & 0 & 1 & 0 \\ 0 & 1 & 0 & 0 \end{bmatrix} \tag{32}$$

N-site and one-particle state Bond dimension with 2 Exact implementation with $O(1)$ depth 2-qubit gate

7 Efficient implementation of CISD state

N-site and 2-particle state (CIS) state Bond dimensions Approximation and numerical calculation of fidelity

Cost of approximation method and comparison against exact one with CCC...-rotation gates.

7.1 Pauli rotation

$$R_x(\theta) = e^{-i\theta X/2} = \begin{bmatrix} \cos(\theta/2) & -i\sin(\theta/2) \\ -i\sin(\theta/2) & \cos(\theta/2) \end{bmatrix} \tag{33}$$

$$R_y(\theta) = e^{-i\theta Y/2} = \begin{bmatrix} \cos(\theta/2) & -\sin(\theta/2) \\ \sin(\theta/2) & \cos(\theta/2) \end{bmatrix} \tag{34}$$

$$R_z(\theta) = e^{-i\theta Z/2} = \begin{bmatrix} e^{-i\theta/2} & 0 \\ 0 & e^{i\theta/2} \end{bmatrix} \tag{35}$$

8 Exchange-type gate

Efficient Symmetry-Preserving State Preparation Circuits for the Variational Quantum Eigensolver Algorithm https://arxiv.org/abs/1904.10910

$$A(\theta,\phi) = \begin{bmatrix} 1 & 0 & 0 & 0 \\ 0 & \cos(\theta) & e^{i\phi}\sin(\theta) & 0 \\ 0 & e^{-i\phi}\sin(\theta) & -\cos(\theta) & 0 \\ 0 & 0 & 0 & 1 \end{bmatrix} \tag{36}$$

$$A(\theta,\phi) = \mathrm{CNOT}_{21}\left(1 \otimes R(\theta,\phi)\right)\mathrm{CNOT}_{12}\left(1 \otimes R^{\dagger}(\theta,\phi)\right)\mathrm{CNOT}_{21}, \tag{37}$$

where

$$\mathrm{CNOT}_{21} = \begin{bmatrix} 1 & 0 & 0 & 0 \\ 0 & 0 & 0 & 1 \\ 0 & 0 & 1 & 0 \\ 0 & 1 & 0 & 0 \end{bmatrix} \tag{38}$$

and

$$R(\theta,\phi) = R_z(\phi+\pi)R_y(\theta+\pi/2) \tag{39}$$

$$\begin{aligned} A(\theta,\phi) &= \mathrm{CNOT}_{21}\begin{bmatrix} R & 0 \\ 0 & R \end{bmatrix}\begin{bmatrix} 1 & 0 \\ 0 & X \end{bmatrix}\begin{bmatrix} R^{\dagger} & 0 \\ 0 & R^{\dagger} \end{bmatrix}\mathrm{CNOT}_{21} && (40) \\ &= \mathrm{CNOT}_{21}\begin{bmatrix} 1 & 0 \\ 0 & RXR^{\dagger} \end{bmatrix}\mathrm{CNOT}_{21} && (41) \\ &= \mathrm{CNOT}_{21}\begin{bmatrix} 1 & 0 \\ 0 & R_zR_yXR_y^{\dagger}R_z^{\dagger} \end{bmatrix}\mathrm{CNOT}_{21} && (42) \end{aligned}$$

$$\begin{aligned} R_yXR_y^{\dagger} &= \begin{bmatrix} \cos(\theta'/2) & -\sin(\theta'/2) \\ \sin(\theta'/2) & \cos(\theta'/2) \end{bmatrix}\begin{bmatrix} 0 & 1 \\ 1 & 0 \end{bmatrix}\begin{bmatrix} \cos(\theta'/2) & \sin(\theta'/2) \\ -\sin(\theta'/2) & \cos(\theta'/2) \end{bmatrix} && (43) \\ &= \begin{bmatrix} -2\sin(\theta'/2)\cos(\theta'/2) & \cos^2(\theta'/2)-\sin^2(\theta'/2) \\ \cos^2(\theta'/2)-\sin^2(\theta'/2) & 2\sin(\theta'/2)\cos(\theta'/2) \end{bmatrix} && (44) \\ &= \begin{bmatrix} -\sin(\theta') & \cos(\theta') \\ \cos(\theta') & \sin(\theta') \end{bmatrix} && (45) \\ &= \begin{bmatrix} -\sin(\theta+\pi/2) & \cos(\theta+\pi/2) \\ \cos(\theta+\pi/2) & \sin(\theta+\pi/2) \end{bmatrix} && (46) \\ &= \begin{bmatrix} -\cos(\theta) & -\sin(\theta) \\ -\sin(\theta) & \cos(\theta) \end{bmatrix} && (47) \\ & && (48) \end{aligned}$$

where $\theta' = \theta + \pi/2$.

$$R_z(R_y X R_y^\dagger)R_z^\dagger = \begin{bmatrix} e^{-i\phi'/2} & 0 \\ 0 & e^{i\phi'/2} \end{bmatrix} \begin{bmatrix} -\cos(\theta) & -\sin(\theta) \\ -\sin(\theta) & \cos(\theta) \end{bmatrix} \begin{bmatrix} e^{i\phi'/2} & 0 \\ 0 & e^{-i\phi'/2} \end{bmatrix} \tag{49}$$

$$= \begin{bmatrix} -\cos(\theta) & -e^{-i\phi'}\sin(\theta) \\ -e^{i\phi'}\sin(\theta) & \cos(\theta) \end{bmatrix} \tag{50}$$

$$= \begin{bmatrix} -\cos(\theta) & -e^{-i\phi-i\pi}\sin(\theta) \\ -e^{i\phi+i\pi}\sin(\theta) & \cos(\theta) \end{bmatrix} \tag{51}$$

$$= \begin{bmatrix} -\cos(\theta) & e^{-i\phi}\sin(\theta) \\ e^{i\phi}\sin(\theta) & \cos(\theta) \end{bmatrix} \tag{52}$$

where $\phi' = \phi + \pi$.

$$A(\theta,\phi) = \mathrm{CNOT}_{21} \begin{bmatrix} 1 & 0 \\ 0 & R_z R_y X R_y^\dagger R_z^\dagger \end{bmatrix} \mathrm{CNOT}_{21} \tag{53}$$

$$= \begin{bmatrix} 1 & 0 & 0 & 0 \\ 0 & \cos(\theta) & e^{i\phi}\sin(\theta) & 0 \\ 0 & e^{-i\phi}\sin(\theta) & -\cos(\theta) & 0 \\ 0 & 0 & 0 & 1 \end{bmatrix} \tag{54}$$

8.1 Definition in Qulacs

$$A(\theta,\phi) = \mathrm{CNOT}_{21}\left(1 \otimes R_y(-\phi-\pi/2)R_z(-\theta-\pi)\right)\mathrm{CNOT}_{12}\left(1 \otimes R_z(\theta+\pi)R_y(\phi+\pi/2)\right)\mathrm{CNOT}_{21}, \tag{55}$$

$$R_z X R_z^\dagger = \begin{bmatrix} 0 & e^{i\theta'} \\ e^{-i\theta'} & 0 \end{bmatrix} = \begin{bmatrix} 0 & -e^{i\theta} \\ -e^{-i\theta} & 0 \end{bmatrix} \tag{56}$$

where $\theta' = \theta + \pi$.

$$R_y(R_z X R_z^\dagger)R_y^\dagger = \begin{bmatrix} -\cos(\phi'/2)\sin(\phi'/2)(e^{i\theta}+e^{-i\theta}) & -e^{i\theta}\cos^2(\phi'/2) + e^{-i\theta}\sin^2(\phi'/2) \\ -e^{-i\theta}\cos^2(\phi'/2) + e^{i\theta}\sin^2(\phi'/2) & \cos(\phi'/2)\sin(\phi'/2)(e^{i\theta}+e^{-i\theta}) \end{bmatrix} \tag{57}$$

where $\phi' = \phi + \pi/2$

9 CIS and circuit

9.1 Single-reference CI wave functions

The FCI wave function is often dominated by a single reference configuration, usually the Hartree-Fock state. It is then convenient to think of the FCI wave function as generated from this reference configuration by the application of a linear combination of spin-orbital excitation operators

$$|\mathrm{FCI}\rangle = \left(1 + \sum_{AI} \hat{X}_I^A + \sum_{A>B,I>J} \hat{X}_{IJ}^{AB}\right) |\mathrm{HF}\rangle \tag{58}$$

where, for example,

$$\hat{X}_I^A |\mathrm{HF}\rangle = C_I^A a_A^\dagger a_I |\mathrm{HF}\rangle \tag{59}$$

$$\hat{X}_{IJ}^{AB} |\mathrm{HF}\rangle = C_{IJ}^{AB} a_A^\dagger a_B^\dagger a_I a_J |\mathrm{HF}\rangle \tag{60}$$

Thus, we may characterize the determinants in the FCI expansion as single (S), double (D), triple (T), quadruple (Q), and higher excitation relative to the Hartree-Fock state.

9.2 CIS

$$|\mathrm{FCI}\rangle = \left(1 + \sum_{AI} \hat{X}_I^A\right) |\mathrm{HF}\rangle = \left(1 + \sum_{AI} C_I^A a_A^\dagger a_I\right) |\mathrm{HF}\rangle \tag{61}$$

9.3 Exact state preparation of CIS on quantum circuit

Applying $R_y(\theta) = e^{i(\theta/2)Y}$ on $|0\rangle$ gives

$$R_y(\theta)|0\rangle = \cos(\theta/2)|0\rangle + \sin(\theta/2)|1\rangle \tag{62}$$

9.3.1 Control-F_y gates

We first define two types of control rotation gates, which we call CF_y^X and CF_y^Z,

$$CF_y^X(\theta) = (1 \otimes R_y(\theta))\mathrm{CNOT}(1 \otimes R_y(-\theta)) = \begin{bmatrix} 1 & 0 \\ 0 & R_y(\theta)XR_y(-\theta) \end{bmatrix}, \tag{63}$$

where

$$\begin{aligned} R_y(\theta)XR_y(-\theta) &= \begin{bmatrix} \cos(\theta/2) & -\sin(\theta/2) \\ \sin(\theta/2) & \cos(-\theta/2) \end{bmatrix} \begin{bmatrix} \sin(-\theta/2) & \cos(-\theta/2) \\ \cos(-\theta/2) & -\sin(-\theta/2) \end{bmatrix} && (64) \\ &= \begin{bmatrix} -2\sin(\theta/2)\cos(\theta/2) & \cos^2(\theta/2) - \sin^2(\theta/2) \\ -\sin^2(\theta/2) + \cos^2(\theta/2) & 2\sin(\theta/2)\cos(\theta/2) \end{bmatrix} && (65) \\ &= \begin{bmatrix} -\sin(\theta) & \cos(\theta) \\ \cos(\theta) & \sin(\theta) \end{bmatrix} && (66) \end{aligned}$$

while

$$CF_y^Z(\theta) = (1 \otimes R_y(\theta))\mathrm{CZ}(1 \otimes R_y(-\theta)) = \begin{bmatrix} 1 & 0 \\ 0 & R_y(\theta)ZR_y(-\theta) \end{bmatrix}, \tag{67}$$

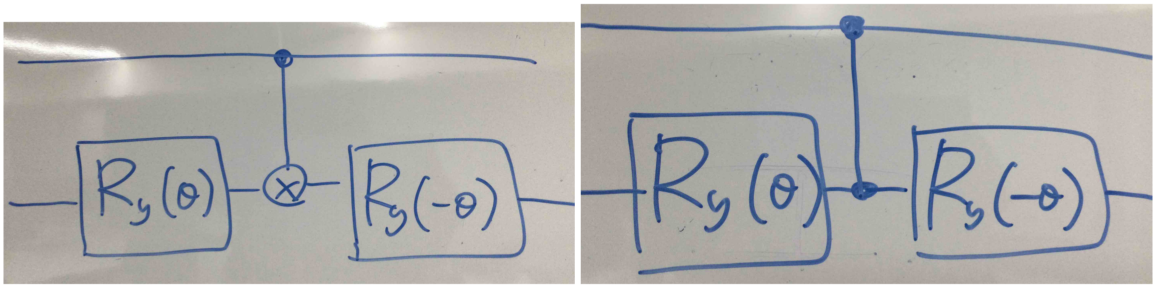

Figure 2: Diagram of CF_y^X gate (left) and CF_y^Z gate (right)

where

$$R_y(\theta) Z R_y(-\theta) = \begin{bmatrix} \cos(\theta/2) & -\sin(\theta/2) \\ \sin(\theta/2) & \cos(\theta/2) \end{bmatrix} \begin{bmatrix} \cos(-\theta/2) & -\sin(-\theta/2) \\ -\sin(-\theta/2) & -\cos(-\theta/2) \end{bmatrix} \tag{68}$$

$$= \begin{bmatrix} \cos^2(\theta/2) - \sin^2(\theta/2) & 2\sin(\theta/2)\cos(\theta/2) \\ 2\sin(\theta/2)\cos(\theta/2) & \sin^2(\theta/2) - \cos^2(\theta/2) \end{bmatrix} \tag{69}$$

$$= \begin{bmatrix} \cos(\theta) & \sin(\theta) \\ \sin(\theta) & -\cos(\theta) \end{bmatrix} \tag{70}$$

Note also that

$$F_y^Z(\theta) |0\rangle = \cos(\theta) |0\rangle + \sin(\theta) |1\rangle \tag{71}$$

$$F_y^X(\theta) |1\rangle = \cos(\theta) |0\rangle + \sin(\theta) |1\rangle \tag{72}$$

We also make use of $C^n(F_y^X)$ gate, which make use of $n-1$ ancilla qubits and $2(n-1)$ Toffoli gates.

9.3.2 Example of 4 spin-orbitals 2 electron state

Consider the case where the number of spin-orbitals $n = 4$ and the number of electrons $m = 2$. Applying the circuit shown in Fig on $|0\rangle^{\otimes 4}$ gives

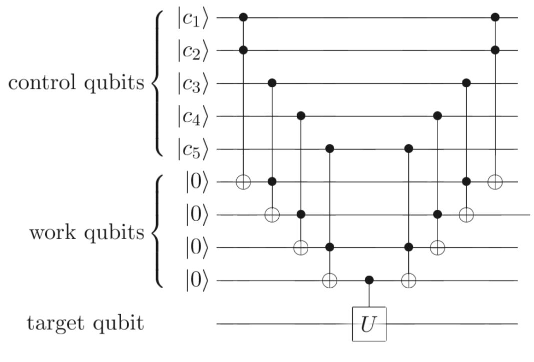

Figure 4.10. Network implementing the $C^n(U)$ operation, for the case $n = 5$.

Figure 3: Implementation of $C^n(U)$ gate

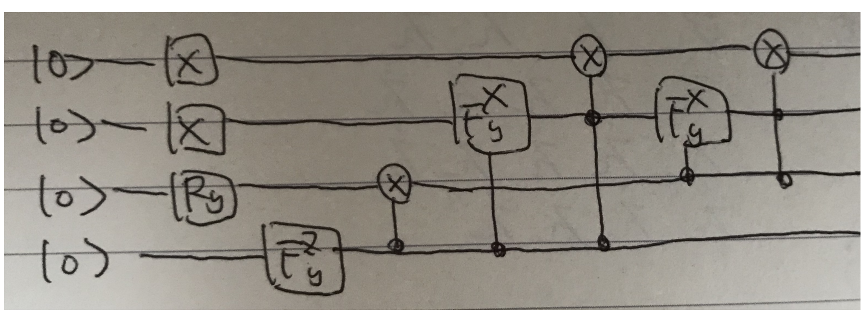

Figure 4: Implementation of circuit which generate CIS state for $(2e, 2o)$

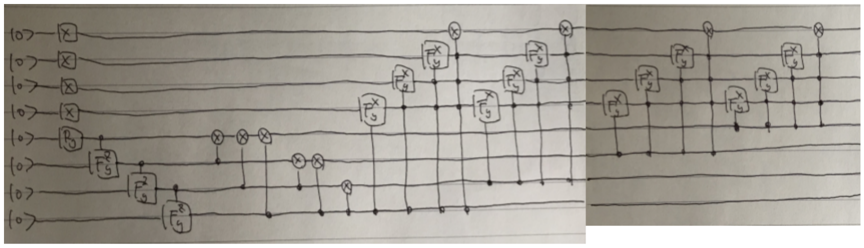

Figure 5: Implementation of circuit which generate CIS state for $(4e, 4o)$

$$
\begin{aligned}
|0\rangle^{\otimes 4} &\xrightarrow{R_y(2\theta_0)X_0X_0} \cos(\theta_0)\,|0011\rangle + \sin(\theta_0)\,|0111\rangle \\
&\xrightarrow{CF_y^Z(\theta_1)} \cos(\theta_0)\,|0011\rangle + \sin(\theta_0)\,(\cos(\theta_1)\,|0111\rangle + \sin(\theta_1)\,|1111\rangle) \\
&\xrightarrow{\text{CNOT}_{32}} \cos(\theta_0)\,|0011\rangle + \sin(\theta_0)\,(\cos(\theta_1)\,|0111\rangle + \sin(\theta_1)\,|1011\rangle) \\
&\xrightarrow{CF_y^X(\theta_2)_{31}} \cos(\theta_0)\,|0011\rangle + \sin(\theta_0)\cos(\theta_1)\,|0111\rangle + \sin(\theta_0)\sin(\theta_1)(\cos(\theta_2)\,|1001\rangle + \sin(\theta_2)\,|1011\rangle) \\
&\xrightarrow{\text{Toffoli}_{310}} \cos(\theta_0)\,|0011\rangle + \sin(\theta_0)\cos(\theta_1)\,|0111\rangle + \sin(\theta_0)\sin(\theta_1)(\cos(\theta_2)\,|1001\rangle + \sin(\theta_2)\,|1010\rangle) \\
&\xrightarrow{CF_y^X(\theta_3)_{21}} \cos(\theta_0)\,|0011\rangle + \sin(\theta_0)\cos(\theta_1)(\cos(\theta_3)\,|0101\rangle + \sin(\theta_3)\,|0111\rangle) + \sin(\theta_0)\sin(\theta_1)(\cos(\theta_2)\,|1001\rangle \\
&\xrightarrow{\text{Toffoli}_{210}} \cos(\theta_0)\,|0011\rangle + \sin(\theta_0)\cos(\theta_1)(\cos(\theta_3)\,|0101\rangle + \sin(\theta_3)\,|0110\rangle) \\
&+ \sin(\theta_0)\sin(\theta_1)(\cos(\theta_2)\,|1001\rangle + \sin(\theta_2)\,|1010\rangle)
\end{aligned}
$$

$$
|\text{CIS}\rangle = \alpha_0\,|0011\rangle + \alpha_1\,|1001\rangle + \alpha_2\,|1010\rangle + \alpha_3\,|0101\rangle + \alpha_4\,|0110\rangle \tag{73}
$$

where

$$
\begin{aligned}
\alpha_0 &= \cos(\theta_0) \\
\alpha_1 &= \sin(\theta_0)\sin(\theta_1)\cos(\theta_2) \\
\alpha_2 &= \sin(\theta_0)\sin(\theta_1)\sin(\theta_2) \\
\alpha_3 &= \sin(\theta_0)\cos(\theta_1)\cos(\theta_3) \\
\alpha_4 &= \sin(\theta_0)\cos(\theta_1)\sin(\theta_3)
\end{aligned}
$$

9.3.3 Example of 8 spin-orbitals 4 electron state

Consider the case where the number of spin-orbitals $n = 8$ and the number of electrons $m = 4$. Applying the circuit shown in Fig on $|0\rangle^{\otimes 8}$ gives CIS state for such electron state.

The circuit can be divided into six parts:

$$
\begin{aligned}
|0\rangle^{\otimes 8} &\xrightarrow{R_{y_4}(2\theta_0)X_3X_2X_1X_0} c_0\,|00001111\rangle + s_0\,|00011111\rangle \\
&\xrightarrow{CF_y^Z(\theta_1)} c_0\,|00001111\rangle + s_0(c_1\,|00011111\rangle + s_1\,|00111111\rangle) \\
&\xrightarrow{CF_y^Z(\theta_2)} c_0\,|00001111\rangle + s_0c_1\,|00011111\rangle + s_0s_1(c_2\,|00111111\rangle + s_2\,|01111111\rangle) \\
&\xrightarrow{CF_y^Z(\theta_3)} c_0\,|00001111\rangle + s_0c_1\,|00011111\rangle + s_0s_1c_2\,|00111111\rangle + s_0s_1s_2(c_3\,|01111111\rangle + s_3\,|11111111\rangle) \\
&= |\psi_1\rangle
\end{aligned}
$$

$$
\begin{aligned}
|\psi_1\rangle &\xrightarrow{\mathrm{CNOT}_{74}\mathrm{CNOT}_{64}\mathrm{CNOT}_{54}} c_0\,|00001111\rangle + s_0c_1\,|00011111\rangle + s_0s_1c_2\,|00101111\rangle \\
&\qquad + s_0s_1s_2(c_3\,|01101111\rangle + s_3\,|11101111\rangle) \\
&\xrightarrow{\mathrm{CNOT}_{65}\mathrm{CNOT}_{75}} c_0\,|00001111\rangle + s_0c_1\,|00011111\rangle + s_0s_1c_2\,|00101111\rangle \\
&\qquad + s_0s_1s_2(c_3\,|01001111\rangle + s_3\,|11001111\rangle) \\
&\xrightarrow{\mathrm{CNOT}_{76}} c_0\,|00001111\rangle + s_0c_1\,|00011111\rangle + s_0s_1c_2\,|00101111\rangle + s_0s_1s_2(c_3\,|01001111\rangle + s_3\,|10001111\rangle) \\
&= |\psi_2\rangle
\end{aligned}
$$

$$
\begin{aligned}
|\psi_2\rangle &\xrightarrow{CF_y^X(\theta_4)} c_0\,|00001111\rangle + s_0c_1\,|00011111\rangle + s_0s_1c_2\,|00101111\rangle + s_0s_1s_2c_3\,|01001111\rangle \\
&\qquad + s_0s_1s_2s_3(c_4\,|10000111\rangle + s_4\,|10001111\rangle) \\
&\xrightarrow{C^2F_y^X(\theta_5)} c_0\,|00001111\rangle + s_0c_1\,|00011111\rangle + s_0s_1c_2\,|00101111\rangle + s_0s_1s_2c_3\,|01001111\rangle \\
&\qquad + s_0s_1s_2s_3c_4\,|10000111\rangle + s_0s_1s_2s_3s_4(c_5\,|10001011\rangle + s_5\,|10001111\rangle) \\
&\xrightarrow{C^3F_y^X(\theta_6)} c_0\,|00001111\rangle + s_0c_1\,|00011111\rangle + s_0s_1c_2\,|00101111\rangle + s_0s_1s_2c_3\,|01001111\rangle \\
&\qquad + s_0s_1s_2s_3c_4\,|10000111\rangle + s_0s_1s_2s_3s_4c_5\,|10001011\rangle \\
&\qquad + s_0s_1s_2s_3s_4s_5(c_6\,|10001101\rangle + s_6\,|10001111\rangle) \\
&\xrightarrow{\mathrm{Toffoli}_{73210}} c_0\,|00001111\rangle + s_0c_1\,|00011111\rangle + s_0s_1c_2\,|00101111\rangle + s_0s_1s_1c_3\,|01001111\rangle \\
&\qquad + s_0s_1s_2s_3c_4\,|10000111\rangle + s_0s_1s_2s_3s_4c_5\,|10001011\rangle \\
&\qquad + s_0s_1s_2s_3s_4s_5(c_6\,|10001101\rangle + s_6\,|10001110\rangle) \\
&= |\psi_3\rangle
\end{aligned}
$$

$$
\begin{aligned}
|\psi_3\rangle \xrightarrow{CF_y^X(\theta_7)} & c_0 |00001111\rangle + s_0c_1 |00011111\rangle + s_0s_1c_2 |00101111\rangle + s_0s_1s_2c_3(c_7 |01000111\rangle + s_7 |01001111\rangle) \\
& + s_0s_1s_2s_3c_4 |10000111\rangle + s_0s_1s_2s_3s_4c_5 |10001011\rangle \\
& + s_0s_1s_2s_3s_4s_5(c_6 |10001101\rangle + s_6 |10001110\rangle) \\
\xrightarrow{C^2F_y^X(\theta_8)} & c_0 |00001111\rangle + s_0c_1 |00011111\rangle + s_0s_1c_2 |00101111\rangle + s_0s_1s_2c_3c_7 |01000111\rangle \\
& + s_0s_1s_2c_3s_7(c_8 |01001011\rangle + s_8 |01001111\rangle) + s_0s_1s_2s_3c_4 |10000111\rangle \\
& + s_0s_1s_2s_3s_4c_5 |10001011\rangle + s_0s_1s_2s_3s_4s_5(c_6 |10001101\rangle + s_6 |10001110\rangle) \\
\xrightarrow{C^3F_y^X(\theta_9)} & c_0 |00001111\rangle + s_0c_1 |00011111\rangle + s_0s_1c_2 |00101111\rangle + s_0s_1s_2c_3c_7 |01000111\rangle \\
& + s_0s_1s_2c_3s_7c_8 |01001011\rangle + s_0s_1s_2c_3s_7s_8(c_9 |01001101\rangle + s_9 |01001111\rangle) \\
& + s_0s_1s_2s_3c_4 |10000111\rangle + s_0s_1s_2s_3s_4c_5 |10001011\rangle \\
& + s_0s_1s_2s_3s_4s_5(c_6 |10001101\rangle + s_6 |10001110\rangle) \\
\xrightarrow{\text{Toffoli}_{63210}} & c_0 |00001111\rangle + s_0c_1 |00011111\rangle + s_0s_1c_2 |00101111\rangle + s_0s_1s_2c_3c_7 |01000111\rangle \\
& + s_0s_1s_2c_3s_7c_8 |01001011\rangle + s_0s_1s_2c_3s_7s_8(c_9 |01001101\rangle + s_9 |01001110\rangle) \\
& + s_0s_1s_2s_3c_4 |10000111\rangle + s_0s_1s_2s_3s_4c_5 |10001011\rangle \\
& + s_0s_1s_2s_3s_4s_5(c_6 |10001101\rangle + s_6 |10001110\rangle) \\
= |\psi_4\rangle &
\end{aligned}
$$

$$
\begin{aligned}
|\psi_4\rangle \xrightarrow{CF_y^X(\theta_{10})}\ & c_0\,|00001111\rangle + s_0c_1\,|00011111\rangle + s_0s_1c_2(c_{10}\,|00100111\rangle + s_{10}\,|00101111\rangle) \\
& + s_0s_1s_2c_3c_7\,|01000111\rangle + s_0s_1s_2c_3s_7c_8\,|01001011\rangle \\
& + s_0s_1s_2c_3s_7s_8(c_9\,|01001101\rangle + s_9\,|01001110\rangle) \\
& + s_0s_1s_2s_3c_4\,|10000111\rangle + s_0s_1s_2s_3s_4c_5\,|10001011\rangle \\
& + s_0s_1s_2s_3s_4s_5(c_6\,|10001101\rangle + s_6\,|10001110\rangle) \\
\xrightarrow{C^2F_y^X(\theta_{11})}\ & c_0\,|00001111\rangle + s_0c_1\,|00011111\rangle + s_0s_1c_2c_{10}\,|00100111\rangle \\
& + s_0s_1c_2s_{10}(c_{11}\,|00101011\rangle + s_{11}\,|00101111\rangle) \\
& + s_0s_1s_2c_3c_7\,|01000111\rangle + s_0s_1s_2c_3s_7c_8\,|01001011\rangle \\
& + s_0s_1s_2c_3s_7s_8(c_9\,|01001101\rangle + s_9\,|01001110\rangle) \\
& + s_0s_1s_2s_3c_4\,|10000111\rangle + s_0s_1s_2s_3s_4c_5\,|10001011\rangle \\
& + s_0s_1s_2s_3s_4s_5(c_6\,|10001101\rangle + s_6\,|10001110\rangle) \\
\xrightarrow{C^3F_y^X(\theta_{12})}\ & c_0\,|00001111\rangle + s_0c_1\,|00011111\rangle + s_0s_1c_2c_{10}\,|00100111\rangle + s_0s_1c_2s_{10}c_{11}\,|00101011\rangle \\
& + s_0s_1c_2s_{10}s_{11}(c_{12}\,|00101101\rangle + s_{12}\,|00101111\rangle) \\
& + s_0s_1s_2c_3c_7\,|01000111\rangle + s_0s_1s_2c_3s_7c_8\,|01001011\rangle \\
& + s_0s_1s_2c_3s_7s_8(c_9\,|01001101\rangle + s_9\,|01001110\rangle) \\
& + s_0s_1s_2s_3c_4\,|10000111\rangle + s_0s_1s_2s_3s_4c_5\,|10001011\rangle \\
& + s_0s_1s_2s_3s_4s_5(c_6\,|10001101\rangle + s_6\,|10001110\rangle) \\
\xrightarrow{\text{Toffoli}_{53210}}\ & c_0\,|00001111\rangle + s_0c_1\,|00011111\rangle + s_0s_1c_2c_{10}\,|00100111\rangle + s_0s_1c_2s_{10}c_{11}\,|00101011\rangle \\
& + s_0s_1c_2s_{10}s_{11}(c_{12}\,|00101101\rangle + s_{12}\,|00101110\rangle) \\
& + s_0s_1s_2c_3c_7\,|01000111\rangle + s_0s_1s_2c_3s_7c_8\,|01001011\rangle \\
& + s_0s_1s_2c_3s_7s_8(c_9\,|01001101\rangle + s_9\,|01001110\rangle) \\
& + s_0s_1s_2s_3c_4\,|10000111\rangle + s_0s_1s_2s_3s_4c_5\,|10001011\rangle \\
& + s_0s_1s_2s_3s_4s_5(c_6\,|10001101\rangle + s_6\,|10001110\rangle) \\
= |\psi_5\rangle &
\end{aligned}
$$

$$
\begin{aligned}
|\psi_5\rangle \xrightarrow{CF_y^X(\theta_{13})}\; & c_0\,|00001111\rangle + s_0c_1(c_{13}\,|00010111\rangle + s_{13}\,|00011111\rangle) + s_0s_1c_2c_{10}\,|00100111\rangle \\
& + s_0s_1c_2s_{10}c_{11}\,|00101011\rangle + s_0s_1c_2s_{10}s_{11}(c_{12}\,|00101101\rangle + s_{12}\,|00101110\rangle) \\
& + s_0s_1s_2c_3c_7\,|01000111\rangle + s_0s_1s_2c_3s_7c_8\,|01001011\rangle \\
& + s_0s_1s_2c_3s_7s_8(c_9\,|01001101\rangle + s_9\,|01001110\rangle) \\
& + s_0s_1s_2s_3c_4\,|10000111\rangle + s_0s_1s_2s_3s_4c_5\,|10001011\rangle \\
& + s_0s_1s_2s_3s_4s_5(c_6\,|10001101\rangle + s_6\,|10001110\rangle) \\
\xrightarrow{C^2F_y^X(\theta_{14})}\; & c_0\,|00001111\rangle + s_0c_1c_{13}\,|00010111\rangle + s_0c_1s_{13}(c_{14}\,|00011011\rangle + s_{14}\,|00011111\rangle) \\
& + s_0s_1c_2c_{10}\,|00100111\rangle + s_0s_1c_2s_{10}c_{11}\,|00101011\rangle \\
& + s_0s_1c_2s_{10}s_{11}(c_{12}\,|00101101\rangle + s_{12}\,|00101110\rangle) \\
& + s_0s_1s_2c_3c_7\,|01000111\rangle + s_0s_1s_2c_3s_7c_8\,|01001011\rangle \\
& + s_0s_1s_2c_3s_7s_8(c_9\,|01001101\rangle + s_9\,|01001110\rangle) \\
& + s_0s_1s_2s_3c_4\,|10000111\rangle + s_0s_1s_2s_3s_4c_5\,|10001011\rangle \\
& + s_0s_1s_2s_3s_4s_5(c_6\,|10001101\rangle + s_6\,|10001110\rangle) \\
\xrightarrow{C^3F_y^X(\theta_{15})}\; & c_0\,|00001111\rangle + s_0c_1c_{13}\,|00010111\rangle + s_0c_1s_{13}c_{14}\,|00011011\rangle \\
& + s_0c_1s_{13}s_{14}(c_{15}\,|00011101\rangle + s_{15}\,|00011111\rangle) \\
& + s_0s_1c_2c_{10}\,|00100111\rangle + s_0s_1c_2s_{10}c_{11}\,|00101011\rangle \\
& + s_0s_1c_2s_{10}s_{11}(c_{12}\,|00101101\rangle + s_{12}\,|00101110\rangle) \\
& + s_0s_1s_2c_3c_7\,|01000111\rangle + s_0s_1s_2c_3s_7c_8\,|01001011\rangle \\
& + s_0s_1s_2c_3s_7s_8(c_9\,|01001101\rangle + s_9\,|01001110\rangle) \\
& + s_0s_1s_2s_3c_4\,|10000111\rangle + s_0s_1s_2s_3s_4c_5\,|10001011\rangle \\
& + s_0s_1s_2s_3s_4s_5(c_6\,|10001101\rangle + s_6\,|10001110\rangle) \\
\xrightarrow{\text{Toffoli}_{43210}}\; & c_0\,|00001111\rangle + s_0c_1c_{13}\,|00010111\rangle + s_0c_1s_{13}c_{14}\,|00011011\rangle \\
& + s_0c_1s_{13}s_{14}(c_{15}\,|00011101\rangle + s_{15}\,|00011110\rangle) \\
& + s_0s_1c_2c_{10}\,|00100111\rangle + s_0s_1c_2s_{10}c_{11}\,|00101011\rangle \\
& + s_0s_1c_2s_{10}s_{11}(c_{12}\,|00101101\rangle + s_{12}\,|00101110\rangle) \\
& + s_0s_1s_2c_3c_7\,|01000111\rangle + s_0s_1s_2c_3s_7c_8\,|01001011\rangle \\
& + s_0s_1s_2c_3s_7s_8(c_9\,|01001101\rangle + s_9\,|01001110\rangle) \\
& + s_0s_1s_2s_3c_4\,|10000111\rangle + s_0s_1s_2s_3s_4c_5\,|10001011\rangle \\
& + s_0s_1s_2s_3s_4s_5(c_6\,|10001101\rangle + s_6\,|10001110\rangle)
\end{aligned}
$$

Here we denote $c_i = \cos(\theta_i)$ and $s_i = \sin(\theta_i)$, and $\text{Toffoli}_{c_1c_2\cdots c_nt}$ as generalized Toffoli gate which has n control qubits $c_1c_2\cdots c_n$.

We see that we obtain

$$
\begin{aligned}
|\mathrm{CIS}\rangle = {} & \alpha_0\,|00001111\rangle + \alpha_1\,|00011110\rangle + \alpha_2\,|00101110\rangle + \alpha_3\,|01001110\rangle + \alpha_4\,|10001110\rangle \\
& + \alpha_5\,|00011101\rangle + \alpha_6\,|00101101\rangle + \alpha_7\,|01001101\rangle + \alpha_8\,|10001101\rangle \\
& + \alpha_9\,|00011011\rangle + \alpha_{10}\,|00101011\rangle + \alpha_{11}\,|01001011\rangle + \alpha_{12}\,|10001011\rangle \\
& + \alpha_{13}\,|00010111\rangle + \alpha_{14}\,|00100111\rangle + \alpha_{15}\,|01000111\rangle + \alpha_{16}\,|10000111\rangle,
\end{aligned}
$$

where

$$
\begin{aligned}
\alpha_0 &= c_0 \\
\alpha_1 &= s_0c_1s_{13}s_{14}s_{15} \\
\alpha_2 &= s_0s_1c_2s_{10}s_{11}s_{12} \\
\alpha_3 &= s_0s_1s_2c_3s_7s_8s_9 \\
\alpha_4 &= s_0s_1s_2s_3s_4s_5s_6 \\
\alpha_5 &= s_0c_1s_{13}s_{14}c_{15} \\
\alpha_6 &= s_0s_1c_2s_{10}s_{11}c_{12} \\
\alpha_7 &= s_0s_1s_2c_3s_7s_8c_9 \\
\alpha_8 &= s_0s_1s_2s_3s_4s_5c_6 \\
\alpha_9 &= s_0c_1s_{13}c_{14} \\
\alpha_{10} &= s_0s_1c_2s_{10}c_{11} \\
\alpha_{11} &= s_0s_1s_2c_3s_7c_8 \\
\alpha_{12} &= s_0s_1s_2s_3s_4c_5 \\
\alpha_{13} &= s_0c_1c_{13} \\
\alpha_{14} &= s_0s_1c_2c_{10} \\
\alpha_{15} &= s_0s_1s_2c_3c_7 \\
\alpha_{16} &= s_0s_1s_2s_3c_4
\end{aligned}
$$

9.3.4 Resource estimation for general cases

Consider the case where the number of qubits n and the number of electrons m. As can be seen from the above examples, we need m X-gates, one R_y-gate, $(n-m-1)$ CF_y^Z gates, $(n-m-1)(n-m)/2$ CNOT gates, $(n-m)$ $CF_y^X, C^2F_y^X, \cdots C^{m-1}F_y^X$ gates, and $(n-m)$ $\text{Toffoli}_{c_1c_2\cdots c_mt}$ gates. Note that each $C^{m-1}F_y^X$ gate consists of $m-1$ ancilla qubits, $2(m-1)$ Toffoli gates and one CF_y^X gate, and each $(n-m)$ $\text{Toffoli}_{c_1c_2\cdots c_mt}$ gate consists of $m-2$ ancilla qubits, $(2m-1)$ Toffoli gates.